Degenerate subspace localization and local symmetries

Peter Schmelcher*

Zentrum für Optische Quantentechnologien, Fachbereich Physik, Universität Hamburg, Luruper Chaussee 149, 22761 Hamburg, Germany and The Hamburg Centre for Ultrafast Imaging, Universität Hamburg, Luruper Chaussee 149, 22761 Hamburg, Germany

(Received 19 January 2024; revised 28 March 2024; accepted 1 April 2024; published 20 May 2024)

Domain specific localization of eigenstates has been a persistent observation for systems with local symmetries. The underlying mechanism for this localization behavior has, however, remained elusive. We provide here an analysis of a local reflection symmetric tight-binding Hamiltonian which attempts at identifying the key features that lead to the localized eigenstates. A weak coupling expansion of closed-form expressions for the eigenvectors demonstrates that the degeneracy of on-site energies occurring at the center of the locally symmetric domains represents the nucleus for eigenstates spreading across the domain. Since the symmetry-related subdomains constituting a locally symmetric domain are isospectral, we encounter pairwise degenerate eigenvalues that split linearly with an increasing coupling strength of the subdomains. The coupling to the (nonsymmetric) environment in an extended setup then leads to the survival of a certain system specific fraction of linearly splitting eigenvalues. The latter go hand in hand with the eigenstate localization on the locally symmetric domain. We provide a brief outlook addressing possible generalizations of local symmetry transformations while maintaining isospectrality.

DOI: 10.1103/PhysRevResearch.6.023188

I. INTRODUCTION

The formation of ordered phases of matter is of major importance for the characterization and understanding of complex quantum systems. This includes highly ordered microscopic structures such as crystal lattices [1], as well as synthetically prepared quantum matter based on, e.g., ultracold neutral atoms in optical lattices [2] or highly excited Rydberg atoms, in arrays of optical tweezers [3]. Symmetries play a crucial role in what state a system adopts, ranging from strongly ordered to completely disordered. In case of geometrical symmetries, each of the well-known symmetries, such as rotation, translation, reflection, or inversion, leave their characteristic fingerprints in the corresponding spectral and eigenstate properties of the underlying quantum system. For global symmetries, i.e., if a symmetry holds for the complete system under investigation, the corresponding group theoretical representation [4] allows us to make powerful predictions beyond the case of system-specific computational studies. If a symmetry is broken globally but retained locally, the powerful toolbox of global symmetry analysis does not apply. The corresponding symmetry operations do not commute with the Hamiltonian since the part of the system where the local symmetry holds is embedded into and coupled to the complementary part of the total system.

Naturally occurring or synthetically prepared setups with local symmetries represent a bridge between global order and disorder. Aperiodic long-range order occurring in quasicrystals fall into the mentioned gap and exhibit a plethora of spatially varying local symmetries [5–14]. Their arrangement is responsible for novel physical properties such as the fractal nature of the energy spectra and the critical localization of the eigenstates. Energy eigenvalues can cluster in so-called quasibands [15–19] that are susceptible to deviations from the perfect aperiodic long-range order. They can develop edge states in case of a finite quasiperiodic sequence [20] which are, in general, remnants of their topological order [16,17].

The consequences of the presence of local symmetries for the theoretical description and simulation of corresponding setups have been pursued intensely in the past decade. In spite of the broken global symmetry, the presence of the local symmetry leads to the existence of invariant nonlocal currents that generalize the parity and Bloch theorem [21–23] for the case of reflection and translation symmetries, respectively. These invariants and their impact on the structure and dynamics have been verified experimentally for both acoustic [24] and optical [25] wave propagation. One of the resulting applications is the classification of scattering resonances based on sum rules for the invariants [26,27]. Systematically introducing more and more local symmetries into an originally disordered chain has been shown to enhance the corresponding transfer efficiency across the chain [28]. An important and always recurring theme and feature of corresponding devices with (many) local symmetries is their eigenstate localization properties on the domains with local symmetries, i.e., LS-domains, in the total system. Specifically, a real space local resonator approach [20] has been developed for binary tight-binding (TB) chains with aperiodic long-range order applying to the situation of

*Peter.Schmelcher@physnet.uni-hamburg.de

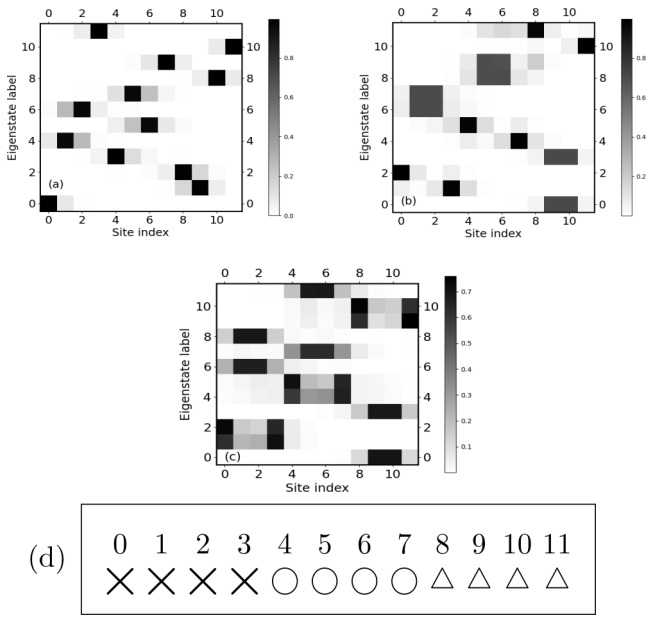

FIG. 1. Eigenstate maps showing the absolute values of the eigenvector components with varying site index (horizontal axis) for an increasing degree of excitation (vertical axis), i.e., an increasing energy, on gray scale for different 12-dimensional TB Hamiltonians. (a) Absence of local symmetries. Diagonal values of the TB Hamiltonian are 0.8,2.4,2.9,5.0,1.9,3.0,2.5,4.0,1.8,0.9,3.1,4.9 and the off-diagonal coupling value is $\epsilon = 0.15$. (b) Three consecutive four-dimensional domains of local reflection symmetry constituting a 12-dimensional TB Hamiltonian for $\epsilon = 0.15$. The diagonal values are 0.8,2.4,2.4,0.8,1.9,3.0,3.0,1.9,3.2,0.9,0.9,3.2, i.e., the LS domains reside on the sites 0–3, 4–7, and 8-11, respectively. (c) Same diagonal values as in (b) but for $\epsilon = 0.45$ for all intradomain couplings and $\epsilon = 0.1$ for all interdomain couplings. (d) shows a sketch of the TB setup indicating the numerically labeled sites within a domain of local symmetry by the same symbols ($\times$, $\bigcirc$, $\bigtriangleup$). This setup belongs to subfigures (b) and (c).

sufficiently strong contrast, i.e., weak to intermediate coupling. This approach can be used to predict the occurrence of gap-edge states and the design of their spectral occurence. Overlapping local symmetries and consequently the "flexible" localization of eigenstates does indeed lead to the bridging of transport across the device [28].

To exemplify the above statements on the interrelation between the presence of local symmetries and the localization properties of the resulting eigenstates, we show in Fig. 1 the eigenstate maps of the absolute values of the eigenvector components for different 12-dimensional TB Hamiltonians. Figure 1(a) shows the case of no local symmetry being present in the Hamiltonian. Obviously for the shown small values of the coupling ϵ, each of the states is strongly localized on its parental zero-coupling site with some smaller amplitude on the left- and right-localized neighboring sites. Figure 1(b) represents the eigenstate map for a setup consisting of three coupled four-dimensional LS domains which reside on the sites 0–3 with on-site values 0.8,2.4,2.4,0.8, sites 4–7 with values 1.9,3.0,3.0,1.9, and sites 8–11 with values 3.2,0.9,0.9,3.2, respectively. Figure 1(d) shows a simple sketch of this setup indicating the numerically labeled sites within a domain of local symmetry by the same symbols ($\times$, $\bigcirc$, $\bigtriangleup$). These LS domains possess a (local) reflection symmetry and each consists of two subdomains which are transformed onto each other by the reflection mapping. As a consequence there exist two neighboring central sites for each LS domain which possess the same on-site energies. The important observation concerning Fig. 1(b) is now that six of the eigenstates show a profile which is distinctly localized on the LS domains, whereas the profile of the others is reminiscent of what we observe in the nonsymmetric case of Fig. 1(a). The local symmetry localized states are not necessarily energetically neighboring states (see the seventh and eighth versus the first and fourth eigenstates).

Finally, Fig. 1(c) shows the same setup like in Fig. 1(b) but now for an off-diagonal coupling that is stronger within an LS domain as compared to between LS domains. As a result the localization onto the LS domains becomes even more pronounced: essentially all eigenstates show this tendency with different degrees of expression.

In spite of the above-exemplified localization properties of eigenstates in the presence of LS domains and their importance for various setups [20,28], a more profound understanding beyond the degenerate perturbation theoretical approach developed in [20] is still lacking. In the present work we address this gap and will develop relevant insights concerning the mechanism for localization in the presence of local symmetries thereby focusing on local reflection symmetries. In Sec. II we perform a weak coupling expansion for the eigenvectors based on a closed form expression provided in Ref. [29]. The resulting eigenvalues and eigenvectors provide us with first indications of the localization properties for small coupling values. In Sec. III we extend this argument on the basis of the fact that subdomains related by a local symmetry operation are isospectral and provide us with pairwise degenerate states that are coupled via the intersubdomain coupling. We provide an evidence-based analysis of the eigenvalue splitting with varying intersubdomain couplings and discuss the case of delocalization within a (sub)domain versus the localization on LS domains. Our conclusions and outlook are provided in Sec. IV.

II. WEAK COUPLING EXPANSION

We will focus in the following on a TB Hamiltonian which takes on the following appearance:

$$\mathcal{H} = \sum_{i=1}^{N} a_i |i\rangle\langle i| + \sum_{\langle i,j\rangle} \epsilon_{ij} |i\rangle\langle j|. \tag{1}$$

We assume, if not explicitly stated otherwise, that the off-diagonal coupling between nearest neighbors $\langle i, j\rangle$ is constant, i.e., $\epsilon_{ij} = \epsilon$ for the complete chain of length N. Specifically, within Sec. II we will always assume a constant off-diagonal coupling. In Sec. III we will, for the purpose of an analysis of the localization behavior due to local symmetries, vary certain off-diagonal couplings while keeping again all others constant. Our choice of the corresponding onsite energies a_i will reflect the absence or presence of local symmetries. Explicit analytical expressions for the eigenvalues and eigenvectors of TB Hamiltonians [30–34] are known only

for special cases, such as tridiagonal Toeplitz matrices, and do not cover the above-given general Hamiltonian (1). However, in Ref. [29] expressions for the squared components $s^2_{\mu i}$ of the normalized eigenvectors have been provided which read as follows:

$$s^2_{\mu i} = \chi_{1:\mu-1}(\lambda^i)\chi_{\mu+1:N}(\lambda^i)/\chi'_{1:N}(\lambda^i), \tag{2}$$

where μ and i refer to the eigenvector component and the label of the eigenstate/eigenenergy. χ represents the characteristic polynomial (CP). $\chi'_{1:N}$ is the derivative of the CP of the complete Hamiltonian matrix. $\chi_{1:\mu-1}(\lambda^i)$ is the CP of the $(\mu-1)\times(\mu-1)$ submatrix obtained by deleting the rows and columns labeled by $\mu, ..., N$ of the complete matrix and taken at the eigenvalue λ^i, correspondingly for $\chi_{\mu+1:N}(\lambda^i)$. While Eq. (2) represents a remarkable and distinguished result, it is of implicit character in the sense that both the knowledge of the exact eigenvalues λ^i and the characteristic polynomial χ are needed to evaluate this expression. To nevertheless exploit the relationship (2) we will perform a weak coupling expansion of both the eigenvalues λ^i and the CPs χ. This will render the above expression (2) explicit and of direct use. Since we focus on a second order expansion w.r.t. the coupling strength ϵ the validity of our approach (within this section) is restricted to small values of ϵ, i.e., weak couplings. This way we will be able to see the onset of the localization behavior due to local symmetries whereas an extension of it will be addressed in the following section.

We expand up to second order in the coupling ϵ (around $\epsilon = 0$) which yields for the eigenvalues $\lambda^i \approx \lambda^i_0 + \epsilon\lambda^i_1 + \epsilon^2\lambda^i_2$ and $\lambda^i_0 = a_i$. For the following derivations we use extensively the recursion relation for the CP [29] providing the CP of the j- dimensional matrix as a function of the CPs of the (j-1)- and (j-2)- dimensional matrices which reads

$$\chi_{1:j}(\lambda) = (\lambda - a_j)\chi_{1:j-1}(\lambda) - \epsilon^2\chi_{1:j-2}. \tag{3}$$

After some algebra, one obtains an explicit expression for the CP valid up to second order of ϵ :

$$\chi_{1:\mu-1}(\lambda^i) = \prod_{j=1}^{\mu-1} X^i_j + \epsilon\lambda^i_1\left(\sum_{j=1}^{\mu-1}\prod_{\substack{k=1\\k\neq j}}^{\mu-1} X^i_k\right) + \epsilon^2\left(\lambda^i_2\sum_{j=1}^{\mu-1}\prod_{\substack{k=1\\k\neq j}}^{\mu-1} X^i_k + {\lambda^i_1}^2\sum_{k=1}^{\mu-2}\sum_{\substack{l=1\\l>k}}^{\mu-1}\prod_{\substack{r=1\\r\neq k,l}}^{\mu-1} X^i_r - \sum_{j=1}^{\mu-2}\prod_{\substack{l=1\\l\neq j,j+1}}^{\mu-1} X^i_l\right), \tag{4}$$

where $X^i_l = (\lambda^i_0 - a_l)$ with $\lambda^i_0 = a_i$. A corresponding expression holds for $\chi_{\mu+1:N}(\lambda^i)$ in Eq. (2). Note that in the above-involved derivation, additional boundary terms appear for the components $\mu \leqslant 3, \mu \geqslant N-2$ which we safely ignore for the following line of argumentation. The denominator $\chi'_{1:N}(\lambda^i)$ in Eq. (2) can be expressed as

$$\chi'_{1:N}(\lambda^i) = \sum_{\mu=1}^{N}\chi_{1:\mu-1}(\lambda^i)\chi_{\mu+1:N}(\lambda^i), \tag{5}$$

where $\chi_{1:0} = \chi_{N+1:N} = 1$. Inserting Eqs. (4) and (5) and the corresponding expression for $\chi_{\mu+1:N}(\lambda^i)$ in Eq. (2) and providing the expansion of the inverse up to second order of ϵ yields for the square of the eigenvector components

$$\begin{aligned} s^2_{\mu i} = &\left(\frac{\mathcal{D}^{(i,0)}_\mu}{\sum_{\nu=1}^{N}\mathcal{D}^{(i,0)}_\nu}\right) + \epsilon\left(\sum_{\nu=1}^{N}\mathcal{D}^{(i,0)}_\nu\right)^{-2}\left(\mathcal{D}^{(i,1)}_\mu\sum_{\nu=1}^{N}\mathcal{D}^{(i,0)}_\nu - \mathcal{D}^{(i,0)}_\mu\sum_{\nu=1}^{N}\mathcal{D}^{(i,1)}_\nu\right) + \epsilon^2\left(\sum_{\nu=1}^{N}\mathcal{D}^{(i,0)}_\nu\right)^{-2} \\ &\times\left(\mathcal{D}^{(i,2)}_\mu\sum_{\nu=1}^{N}\mathcal{D}^{(i,0)}_\nu - \mathcal{D}^{(i,1)}_\mu\sum_{\nu=1}^{N}\mathcal{D}^{(i,1)}_\nu\right) + \epsilon^2\left(\mathcal{D}^{(i,0)}_\mu\right)\left(\sum_{\nu=1}^{N}\mathcal{D}^{(i,0)}_\nu\right)^{-3}\left(\left(\sum_{\nu=1}^{N}\mathcal{D}^{(i,1)}_\nu\right)^2 - \left(\sum_{\nu=1}^{N}\mathcal{D}^{(i,0)}_\nu\right)\left(\sum_{\nu=1}^{N}\mathcal{D}^{(i,2)}_\nu\right)\right), \end{aligned} \tag{6}$$

where

$$\begin{aligned} \mathcal{D}^{(i,0)}_\mu &= \prod_{\substack{j=1\\j\neq\mu}}^{N} X^i_j \qquad \mathcal{D}^{(i,1)}_\mu = \lambda^i_1\left(\sum_{\substack{j=1\\j\neq\mu}}^{N}\prod_{\substack{k=1\\k\neq j,\mu}}^{N} X^i_k\right) \\ \mathcal{D}^{(i,2)}_\mu &= {\lambda^i_1}^2\left(\left(\sum_{j=1}^{\mu-1}\prod_{\substack{k=1\\k\neq j}}^{\mu-1} X^i_k\right)\left(\sum_{j=\mu+1}^{N}\prod_{\substack{k=\mu+1\\k\neq j}}^{N} X^i_k\right) + \left(\sum_{k=1}^{\mu-2}\sum_{\substack{l=1\\l>k}}^{\mu-1} + \sum_{k=\mu+1}^{N-1}\sum_{\substack{l=\mu+1\\l>k}}^{N}\right)\prod_{\substack{j=1\\j\neq\mu,l,k}}^{N} X^i_j\right) \\ &\quad + \lambda^i_2\left(\sum_{\substack{j=1\\j\neq\mu}}^{N}\prod_{\substack{k=1\\k\neq j,\mu}}^{N} X^i_k\right) - \left(\sum_{\substack{j=1\\j\neq\mu-1,\mu}}^{N-1}\prod_{\substack{k=1\\k\neq\mu,j,j+1}}^{N} X^i_k\right). \end{aligned} \tag{7}$$

The first and second order contributions $\lambda^i_k; k = 1, 2; i = 1, ..., N$ to the eigenvalues λ^i are derived on the basis of Eqs. (3) and (4). The CP has been expanded up to second order of ϵ by using the above recursion relation iteratively, and consequently

we equate it to zero. We then demand that the terms of each order of ϵ, namely the "coefficients" of ϵ and ϵ^2 are zero resulting on equations for $\lambda_k^i; k = 1, 2; i = 1, ..., N$.

Let us first focus on the case of a nondegenerate zeroth order spectrum, i.e., all the diagonal elements are pairwise different $a_i \neq a_j$ for $i \neq j$, which corresponds to a situation whose eigenstate map is shown in Fig. 1(a). We obtain $\lambda_1^i = 0 \; \forall \; i$ and only the second order contribution is nonzero. It reads

$$\lambda_2^i = \left(X_{i+1}^i\right)^{-1} + \left(X_{i-1}^i\right)^{-1}. \tag{8}$$

For the corresponding eigenvector one has to distinguish between the original zeroth order site i and the neighboring ones. We therefore obtain

$$\begin{aligned} s_{ii}^2 &= 1 - \epsilon^2 \left(\mathcal{D}_i^{(i,0)}\right)^{-1} \left(\sum_{\nu=1, \nu \neq i}^{N} \mathcal{D}_\nu^{(i,2)} \right), \\ s_{\mu i}^2 &= \epsilon^2 \left(\mathcal{D}_i^{(i,0)}\right)^{-1} \left(\mathcal{D}_\mu^{(i,2)}\right), \quad \mu \neq i. \end{aligned} \tag{9}$$

This demonstrates, as expected, that primarily the zeroth order site is dominantly contributing and the neighboring sites appear in second order of the coupling ϵ as shown in Fig. 1(a). The exact eigenstates possess, of course, contributions of higher order w.r.t. ϵ and are slightly more delocalized.

Let us now address the case of two neighboring sites $i, i+1$ that possess the same on-site energies for zero coupling, and we focus on the eigenvalues of the TB Hamiltonian which emerge from this degenerate pair when increasing the coupling strength. Such a configuration appears if an LS domain based on local reflection is present in the Hamiltonian, as discussed above. We therefore have $\lambda_0^i = \lambda_0^{i+1} = a_i = a_{i+1}$ relating to the two central sites of the LS domain. From the CP we then obtain $\lambda_1^i = -\lambda_1^{i+1} = 1$, i.e., naturally a linear order term appears in the expansion of the eigenvalue(s). Due to the fact that $\mathcal{D}_\mu^{(i,0)} = 0 \; \forall \; \mu$, the expansion in the nominator and the denominator of Eq. (2) start in linear order of ϵ, respectively, and we obtain for the eigenvectors

$$\begin{aligned} s_{\mu\alpha}^2 = \frac{1}{2} + \epsilon &\left(\sum_{\nu=1}^{N} \mathcal{D}_\nu^{(\alpha,1)} \right)^{-2} \\ &\left(\mathcal{D}_\mu^{(\alpha,2)} \left(\sum_{\nu=1}^{N} \mathcal{D}_\nu^{(\alpha,1)} \right) - \mathcal{D}_\mu^{(\alpha,1)} \left(\sum_{\nu=1}^{N} \mathcal{D}_\nu^{(\alpha,2)} \right) \right) \quad \text{for } \alpha, \mu \in [i, i+1], \end{aligned} \tag{10a}$$

$$s_{\mu\alpha}^2 = \epsilon \left(\sum_{\nu=1}^{N} \mathcal{D}_\nu^{(\alpha,1)} \right)^{-1} \mathcal{D}_\mu^{(\alpha,2)} \quad \text{for } \alpha \in [i, i+1], \mu \notin [i, i+1]. \tag{10b}$$

Equations (10a) and (10b) show that the central two sites with equal on-site energy possess in leading order the same values $\frac{1}{2}$ for the corresponding squared eigenvector components. This can be interpreted as follows. The degenerate zeroth order pair $i, i+1$ with on-site values $a_i = a_{i+1}$ forms a "nucleus" for the localization of the corresponding eigenvectors on the LS domain. Moving outward from this nucleus within the LS domain, further next order contributions to the corresponding eigenvector components appear, see Eq. (10b), that have a corresponding counterpart for the central components, see Eq. (10a) [35]. As far as we can judge within the weak coupling expansion up to second order ϵ^2, the central on-site energy degeneracy represents the seed for the localization of the eigenvectors on the LS domains. In the next section we will explore the more general case of higher-order effects and/or stronger couplings based on the argument of a pairwise degeneracy of all eigenstates within an isolated LS domain. This will provide us with even stronger arguments for the localization mechanism at work. A final note is in order concerning the above weak coupling expansion. In principle, a higher order expansion follows the same procedure. However, the corresponding algebraic manipulations become tedious and, therefore, a computer algebraic approach might be more feasible.

III. DEGENERATE SUBSPACE LOCALIZATION

Let us now consider a broader range of values for the coupling ϵ but still staying in the regime of a strong contrast $\frac{a_i - a_{i+1}}{\epsilon} > 1$ for $a_i \neq a_{i+1}$. If the contrast would be significantly smaller than one, the tendency of delocalization for all eigenstates would smear them out and, consequently, the impact of the LS domains on the localization becomes negligible. Naturally, since analytical calculations are not possible in this regime, we base our analysis on the results of numerical simulations. To begin with we focus on a single LS domain consisting of two subdomains that are mapped onto each other by a (local) symmetry operation and we assume (as always) open boundary conditions. Let us assume that the center coupling (i.e., intersubdomain coupling) between the two subdomains is zero, i.e., $\epsilon_c = 0$. In case of a translation, the two submatrices belonging to the two subdomains are identical and, in particular, isospectral, i.e., they possess identical eigenvalues. Of course, they also possess the same eigenvectors. This isospectrality holds also for a reflection operation. The latter can be proven by performing $\lfloor \frac{N}{2} \rfloor$ exchange operations of the columns and subsequently of the rows from the outside to the inside of the original submatrix which yields the submatrix of the symmetry transformed subdomain

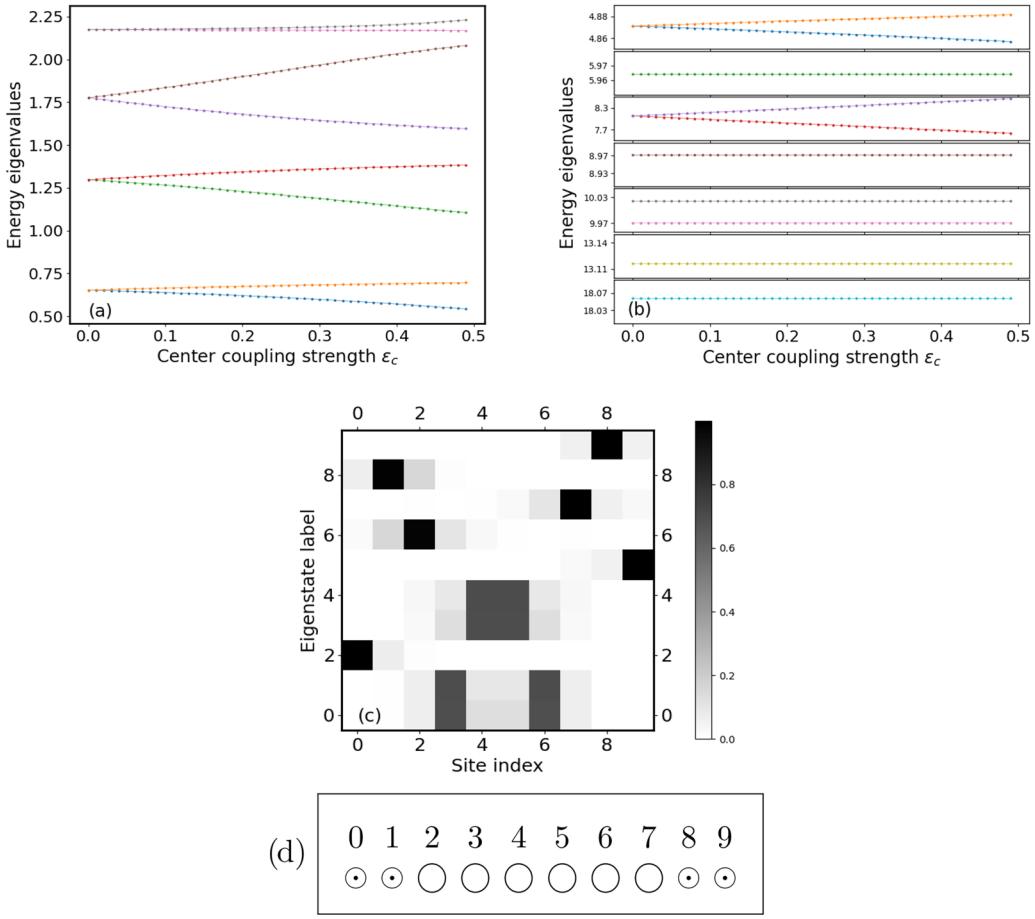

FIG. 2. Energy eigenvalue spectra (a,b) for a varying center coupling value $\epsilon_c = 0 - 0.5$. (a) A single reflection LS domain consisting of eight sites and a subdomain coupling strength $\epsilon = 0.4$. Diagonal values of the TB-Hamiltonian are 1.9,1.4,1.1,1.5,1.5,1.1,1.4,1.9. We observe the pairwise degeneracy of the eigenvalues for $\epsilon_c = 0$ and their linear splitting with increasing value of ϵ_c (note that this splitting is very small for the pair with the largest eigenvalues and barely visible on the scale of the figure). (b) A stack of subfigures showing the eigenvalue spectrum for a single reflection LS domain embedded into an asymmetric environment. Diagonal values of the ten-dimensional TB-Hamiltonian are 6.0,13.0,10.0,5.0,8.0,8.0,5.0,10.0,18.0,9.0, containing a six-dimensional reflection symmetric domain. As for (a) the center coupling obeys $\epsilon_c = 0 - 0.5$ and the remaining couplings are $\epsilon = 0.5$. (c) The eigenstate map of the setup (b) for $\epsilon_c = \epsilon = 0.5$. Eigenvector components are shown with varying site index on the horizontal axis, and sorted w.r.t. increasing energy eigenvalues from bottom to top along the vertical axis. (d) shows a sketch of the TB setup indicating the numerically labeled sites and the domain with local symmetry by the symbol ◯ and the nonsymmetric sites/domains with the symbol ⊙, all over belonging to subfigures (b) and (c).

and makes up for a total sign change of $(-1)^{2\cdot\lfloor\frac{N}{2}\rfloor} = +1$ of the corresponding determinant. The corresponding eigenvector components for the two subdomains are related by $s_{ji} = s_{N-j+1\,i}$. The above implies that the spectrum consists of pairs of degenerate eigenvalues for $\epsilon_c = 0$, independent of the strength of the intrasubdomain coupling ϵ. With increasing value of the coupling ϵ, the subdomain eigenstates become increasingly delocalized inside the subdomain.

The center coupling ϵ_c represents a key quantity for the analysis of the spectral and eigenstate properties since it couples isospectral submatrices and, importantly, since it maintains the symmetry properties of the setup while being varied.

As a consequence of the above discussed properties, we observe that all pairwise degenerate eigenvalues of the decoupled subdomains split linearly if we increase their center coupling strength ϵ_c starting from a zero value. Figure 2(a) shows an eight-dimensional case for the on-site values 1.9,1.4,1.1,1.5,1.5,1.1,1.4,1.9, and $\epsilon = 0.4$. For a given on-site energy configuration, the strength of the splitting increases with an increasing value for the subdomain coupling strength ϵ. For larger values of ϵ_c a nonlinear behavior takes over. Let us now bring a reflection symmetric domain in contact with an asymmetric environment, as sketched in Fig. 2(d). The resulting eigenvalue spectrum is shown in Fig. 2(b) for the case of a six-dimensional reflection symmetric domain with diagonal values 10.0,5.0,8.0,8.0,5.0,10.0 in contact with two left and two right attached asymmetric sites. There are two main effects we consequently observe.

First the symmetry breaking leads to an energy splitting of the originally degenerate pair for $\epsilon_c = 0$ which is tiny for the central neighboring sites but increases significantly for pairs located closer to the boundaries of the LS domain. Second there is still large intervals of ϵ_c for which the two inner of the three pairs of the LS domain show an approximate linear splitting and dependence on ϵ_c. The other eigenvalues

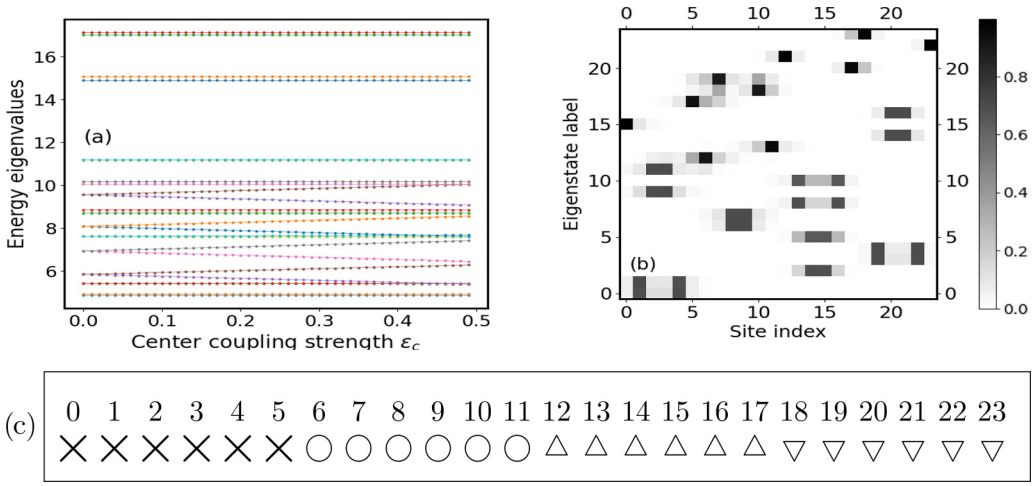

FIG. 3. A 24-dimensional TB Hamiltonian consisting of four different six-dimensional neighboring reflection-based LS domains. The four domains involve the sites [0–5], [6–11], [12–17], [18–23]. (a) Energy eigenvalue spectra with varying (all four) center coupling strengths $\epsilon_c = 0 - 0.5$. (b) The corresponding eigenstate map for $\epsilon = \epsilon_c = 0.5$. (c) shows a sketch of the TB setup indicating the numerically labeled sites and drawing sites within domains with a local symmetry by the same symbols ($\times$, $\bigcirc$, $\triangle$, $\triangledown$).

show a behavior which is (on the shown scale) insensitive to the variations of ϵ_c. Figure 2(c) shows the same setup as in Fig. 2(b) and, for $\epsilon_c = \epsilon = 0.5$, the corresponding eigenstate map. There are four low energy eigenstates which are localized on the LS domain and show dominant values on two sites. These correspond to the eigenvalues that show a linear splitting in Fig. 2(b). The other eigenstates show a dominant single site behavior, as ubiquitous in the absence of any (local) symmetry.

Note that the coupling ϵ in the subdomains plays an important role in the above discussed behavior: it helps delocalizing the eigenstates on the subdomain leading to a stronger sensitivity w.r.t. the center coupling ϵ_c and, consequently, an enforced localization on the LS domain overall. This argument has to be taken with a grain of salt, since making the coupling too strong yields an overall delocalization not "seeing the particular imprint" of the LS domain at all.

Figures 3(a) and 3(b) show the eigenvalue spectrum and an eigenstate map for a more complex setup: a 24-site Hamiltonian with four different six-dimensional reflection-symmetric domains, which is sketched in Fig. 3(c). We observe again a substantial subset of linearly splitting eigenvalues [for some of them the splitting is not visible on the scale of Fig. 3(a)], all with varying center couplings ϵ_c. The corresponding eigenstate map in Fig. 3(b) shows that 14 out of the 24 eigenstates are confined to LS domains and follow their characteristic profile.

IV. CONCLUSIONS AND OUTLOOK

Breaking global symmetries and retaining them locally leads directly to a plethora of possible setups that fall into the gap between perfect order and complete disorder. The quest for the characterization of the properties of such systems is of immediate interest in view of the fact that there are many different ways of implementing local symmetries: they could be, e.g., isolated, neighboring, overlapping, and covering or non-covering in terms of their domains. In the present work we make an attempt to better understand the eigenstate localization behavior of locally symmetric Hamiltonians which has been observed in previous works such as Refs. [20,23]. In those works it has consistently been monitored that a certain significant portion of the eigenstates prefers to localize, i.e., have their dominant eigenvector components, on locally symmetric domains of the total setup. Therefore, one can use the freedom of incorporating local symmetries in a "device" to steer the localization behavior of the corresponding eigenstates.

We have been focusing on local reflection symmetries to analyze the spectrum of eigenvalues and eigenstates. Our first analysis step was based on the closed form expressions for the eigenvectors of the tight-binding Hamiltonian provided in Ref. [29]. While these expressions involve the exact characteristic polynomial and eigenvalues, a weak coupling expansion renders them of immediate use within a low order series approximation of the coupling strength. If no local symmetries are present we obtain the expected single site dominant behavior for the eigenvectors, with some small amplitude on neighboring sites. It is the degeneracy of the zeroth order eigenvalues at the center of a local reflection symmetric domain which serves as a nucleus for the eigenvector delocalization on locally symmetric domains in the weak coupling limit.

To address the regime of larger values for the couplings, but still remaining within the range of a strong contrast, we numerically explored for several examples the spectral behavior of the eigenvalues and their eigenstate localization in the presence of one or several local symmetries. Our first observation was the fact that mapping a subdomain via a reflection operation onto its image subdomain is an operation which maintains the underlying eigenvalues of the corresponding Hamiltonian, i.e., the two subdomain Hamiltonians are isospectral independently of the value of the coupling strength within the subdomain. As a consequence, for zero center coupling between the subdomains we encounter degenerate pairs of eigenvalues. Switching on the center coupling leads to a linear splitting of all pairwise degenerate eigenvalues if

there is no coupling to an (asymmetric) environment, i.e., to neighboring sites. The case of interest is the one for which a locally symmetric domain is embedded into a larger setup. Then it is only a subset of the eigenvalues which split linearly, depending on the strength of the coupling to the environment. This holds for each locally symmetric domain separately. Our analysis of the eigenstates via eigenstate maps reflects the correlation between the linear splitting and the localization of the eigenstates on domains with local symmetries. The coupling to the environment weakens the localization tendency on the underlying locally symmetric domains: from the surface of the domains to their center this process becomes less pronounced.

While the above facts illuminate the origin and mechanism of the ubiquitously observed localization of eigenstates in the framework of setups exhibiting local symmetries, it also opens up new perspectives. In our approach the key ingredient is the isospectrality of the two subdomains constituting the locally symmetric domain. One could now choose as subdomains not symmetry related ones, but an original subdomain and a similarly transformed one. By construction, both subdomains possess the same set of eigenvalues. It is then an open question to what extent and under what (additional) criteria the coupled subdomains would show, once embedded into an environment, corresponding localization properties. In this context it is an intriguing perspective to explore the recently investigated latent or hidden symmetries [36–38] which are based on isospectral reduction techniques of spectral graph theory [39–41], thereby generalizing the here studied local symmetries.

ACKNOWLEDGMENTS

P.S. acknowledges fruitful discussions with J. Schirmer on degenerate perturbation theory and with M. Röntgen on the impact of local symmetries. This work has been supported by the Cluster of Excellence "Advanced Imaging of Matter,, of the Deutsche Forschungsgemeinschaft (DFG)-EXC 2056, Project ID No. 390715994.

[1] H. Bruus and K. Flensberg, *Many-body Quantum Theory in Condensed Matter Physics: An Introduction*, Oxford Graduate Texts (Oxford University Press, Oxford, 2004).

[2] I. Bloch, J. Dalibard, and W. Zwerger, Many-body physics with ultracold gases, Rev. Mod. Phys. **80**, 885 (2008).

[3] A. Browaeys and T. Lahaye, Many-body physics with individually controlled Rydberg atoms, Nat. Phys. **16**, 132 (2020).

[4] M. Hamermesh, *Group Theory and Its Applications to Physical Problems*, Dover Books on Physics and Chemistry (Dover Publications, Mineola, NY, 1989).

[5] E. Maciá Barber, *Aperiodic Structures in Condensed Matter, Fundamentals and Applications*, Series in Condensed Matter Physics (CRC Press, Boca Raton, FL, 2009).

[6] E. Maciá-Barber, *Quasicrystals, Fundamentals and Applications* (CRC Press, Boca Raton, FL, 2021).

[7] D. Shechtman, I. Blech, D. Gratias, and J. W. Cahn, Metallic phase with long-range orientational order and no translational symmetry, Phys. Rev. Lett. **53**, 1951 (1984).

[8] J. B. Suck, M. Schreiber, and P. Häussler, *Quasicrystals: An Introduction to Structure, Physical Properties and Applications* (Springer Science & Business Media, New York, 2002).

[9] T. Janssen, Crystallography of quasi-crystals, Acta Crystallogr **42**, 261 (1986).

[10] C. Berger, T. Grenet, P. Lindqvist, P. Lanco, J. Grieco, G. Fourcaudot, and F. Cyrot-Lackmann, The new AlPdRe icosahedral phase: Towards universal electronic behaviour for quasicrystals? Solid State Commun. **87**, 977 (1993).

[11] A. P. Vieira, Low-energy properties of aperiodic quantum spin chains, Phys. Rev. Lett. **94**, 077201 (2005).

[12] D. Tanese, E. Gurevich, F. Baboux, T. Jacqmin, A. Lemaitre, E. Galopin, I. Sagnes, A. Amo, J. Bloch, and E. Akkermans, Fractal energy spectrum of a polariton gas in a Fibonacci quasiperiodic potential, Phys. Rev. Lett. **112**, 146404 (2014).

[13] A. Jagannathan, The Fibonacci quasicrystal: Case study of hidden dimensions and multifractality, Rev. Mod. Phys. **93**, 045001 (2021).

[14] C. Morfonios, P. Schmelcher, P. A. Kalozoumis, and F. K. Diakonos, Local symmetry dynamics in one-dimensional aperiodic lattices: a numerical study, Nonlinear Dyn **78**, 71 (2014).

[15] E. de Prunelé and X. Bouju, Fibonacchi, Koch and Penrose structures: Spectrum of finite subsystems in three-dimensional space, Phys. Status Solidi B **225**, 95 (2001).

[16] E. de Prunelé, Penrose structures: Gap labeling and geometry, Phys. Rev. B **66**, 094202 (2002).

[17] M. A. Bandres, M. C. Rechtsman, and M. Segev, Topological photonic quasicrystals: Fractal topological spectrum and protected transport, Phys. Rev. X **6**, 011016 (2016).

[18] P. Vignolo, M. Bellec, J. Böhm, A. Camara, J. M. Gambaudo, U. Kuhl, and F. Mortessagne, Energy landscape in a Penrose tiling, Phys. Rev. B **93**, 075141 (2016).

[19] E. Maciá, Clustering resonance effects in the electronic energy spectrum of tridiagonal Fibonacchi quasicrystals, Phys. Status Solidi B **254**, 1700078 (2017).

[20] M. Röntgen, C. V. Morfonios, R. Wang, L. Dal Negro, and P. Schmelcher, Local symmetry theory of resonator structures for the real-space control of edge states in binary aperiodic chains, Phys. Rev. B **99**, 214201 (2019).

[21] P. A. Kalozoumis, C. Morfonios, F. K. Diakonos and P. Schmelcher, Invariant of broken discrete symmetries, Phys. Rev. Lett. **113**, 050403 (2014).

[22] P. Schmelcher, S. Krönke, and F. K. Diakonos, Dynamics of local symmetry correlators for interacting many-particle systems, J. Chem. Phys. **146**, 044116 (2017).

[23] C. Morfonios, P. A. Kalozoumis, F. K. Diakonos and P. Schmelcher, Nonlocal discrete continuity and invariant currents in locally symmetric effective Schrödinger arrays, Ann. Phys. **385**, 623 (2017).

[24] P. A. Kalozoumis, O. Richoux, F. K. Diakonos, G. Theocharis, and P. Schmelcher, Invariant currents in lossy acoustic waveguides with complete local symmetry, Phys. Rev. B **92**, 014303 (2015).

[25] N. Schmitt, S. Weimann, C. V. Morfonios, M. Röntgen, M. Heinrich, P. Schmelcher, and A. Szameit, Observation of local symmetry in photonic systems, Laser Photon. Rev. **14**, 1900222 (2020).

[26] P. A. Kalozoumis, C. Morfonios, F. K. Diakonos, and P. Schmelcher, Local symmetries in one-dimensional quantum scattering, Phys. Rev. A **87**, 032113 (2013).

[27] P. A. Kalozoumis, C. Morfonios, N. Palaiodimopoulos, F. K. Diakonos, and P. Schmelcher, Local symmetries and perfect transmission in aperiodic photonic multilayers, Phys. Rev. A **88**, 033857 (2013).

[28] C. V. Morfonios, M. Röntgen, F. K. Diakonos, and P. Schmelcher, Transfer efficiency enhancement and eigenstate properties in locally symmetric disordered finite chains, Ann. Phys. **418**, 168163 (2020).

[29] B. N. Parlett, *The Symmetric Eigenvalue Problem*, SIAM Classics in Applied Mathematics Series, Vol. 20 (SIAM, Philadelphia, 1998).

[30] S. Kouachi, Eigenvalues and eigenvectors of tridiagonal matrices, El. J. Lin. Alg. **15**, 115 (2006).

[31] D. Kulkarni, D. Schmidt, and S.-K. Tsui, Eigenvalues of tridiagonal pseudo-Toeplitz matrices, Linear Algebra Appl. **297**, 63 (1999).

[32] A. R. Willms, Analytic results for the eigenvalues of certain tridiagonal matrices, SIAM J. Matrix Anal. Appl. **30**, 639 (2008).

[33] S. Noschese, L. Pasquini, and L. Reichel, Tridiagonal Toeplitz matrices: properties and novel applications, Numerical Linear Algebra App. **20**, 302 (2013).

[34] Y. Nakatsukasa, Eigenvalue perturbation bounds for Hermitian block tridiagonal matrices, Appl. Numer. Math. **62**, 67 (2012).

[35] We remark that our line of argumentation is valid independently of the definite order $\mathcal{O}(\epsilon^n)$ which appears to be nonzero besides the constant value $\frac{1}{2}$ in Eqs. (10a) and (10b).

[36] M. Röntgen, M. Pyzh, C. V. Morfonios, N. E. Palaiodimopoulos, F. K. Diakonos, and P. Schmelcher, Latent symmetry induced degeneracies, Phys. Rev. Lett. **126**, 180601 (2021).

[37] C. V. Morfonios, M. Röntgen, M. Pyzh, and P. Schmelcher, Flat bands by latent symmetry, Phys. Rev. B **104**, 035105 (2021).

[38] M. Röntgen, C. V. Morfonios, P. Schmelcher, and V. Pagneux, Hidden symmetries in acoustic wave systems, Phys. Rev. Lett. **130**, 077201 (2023).

[39] D. Smith and B. Webb, Hidden symmetries in real and theoretical networks, Physica A **514**, 855 (2019).

[40] L. Bunimovich and B. Webb, *Isospectral Transformations: A New Approach to Analyzing Multidimensional Systems and Networks*, 1st ed., Springer Monographs in Mathematics (Springer, New York, 2014).

[41] M. Kempton, J. Sinkovic, D. Smith, and B. Webb, Characterizing cospectral vertices via isospectral reduction, Linear Algebra Appl. **594**, 226 (2020).